Journal of Electrostatics 93 (2018) 85–96

Contents lists available at ScienceDirect

Journal of Electrostatics

journal homepage: www.elsevier.com/locate/elstat

Ionic wind produced by positive and negative corona discharges in air

Eric Moreau*, Pierre Audier, Nicolas Benard

University of Poitiers, Pprime Institute, CNRS, ISAE-ENSMA, Téléport 2, BP 30179, 86962 Futuroscope, France

A B S T R A C T

In this experimental study, we aimed at better understanding the electrohydrodynamic phenomena occurring inside positive and negative point-to-plate corona discharges in atmospheric air. First, electrical and optical measurements allowed us to observe the different discharge regimes according to the voltage polarity; the Hermstein's glow regime and then the breakdown streamer one in the case of a positive corona, and the Trichel pulse regime and then the pulseless one for the negative corona. More, we highlighted that the discharge current always follows the theoretical Townsend's expression, except in one case. Indeed, for the positive corona, the discharge current starts to evolve linearly with the voltage when the streamer regime appears. Secondly, the time-averaged and time-resolved velocity of the ionic wind has been characterized by high speed particle imaging velocimetry. We observed that when the high voltage is switched on, a jet starts from the needle and then its moves toward the plate, resulting in a wall-impinging jet with a vortex ring. Moreover, we highlighted that a negative corona discharge produces a steady ionic wind with weak velocity fluctuations. On the contrary, the positive discharge induces a faster ionic wind, showing that it is more efficient than the negative discharge in ionic wind production, more especially when the breakdown streamer regime appears. Indeed, in this case, the mean velocity becomes constant along the x axis, meaning that there is still a EHD force in the inter-electrode gap, which is able to counter the viscous effects.

1. Introduction

When a high potential difference is applied between two electrodes in atmospheric air, ionization of the air molecules around the thinnest electrode induces a corona discharge. Due to the electric field, these ions are submitted to Coulomb force, resulting in their motion from the active electrode toward the grounded collecting one. The set of all these Coulomb forces results in a volume electrohydrodynamic (EHD) force occurring inside the discharge. Hence, in the electrode gap, many collisions between ions in motion and neutral air molecules take place, resulting in a momentum transfer that produces a gas flow, which is usually called “ionic wind”.

Important studies on the physics of corona discharges started at the end of the 19th century [1,2] and continued throughout the 20th century [3–19]. Although they involve complex electrical, chemical and mechanical phenomena, they are easy to enforce. Therefore, they are used in numerous engineering applications, such as ozone production [20,21], reduction of gaseous pollutants [22,23], surface treatment [24], assisted-combustion [25,26], electrostatic precipitation [27–29] and thrust production [30,31] for instance.

In the present paper, we focus on the electrohydrodynamic phenomena occurring inside corona discharges in atmospheric air. The first publication dedicated to this subject is the one of Chattok [2] in 1899, but we can say that theory of EHD in gas started with the well-known publication of Robinson [32] in 1961 that investigated the ability of corona discharges to perfect blowers in absence of any moving mechanical part. More recently, for about 10 years, several others research groups have been studying corona discharges, with the aim at increasing the electric wind velocity, the resulting flow rate and the electromechanical efficiency of such devices [33–37]. However, only few studies have been devoted to a better understanding of the physical phenomena occurring inside the discharge and the complex plasma-gas interaction.

Hence, in the present paper, we propose to detail the ionic wind produced when the discharge is ignited, and to compare negative and positive coronas. For that purpose, we have developed a multi-metrology experimental bench including electrical measurements, iCCD visualizations and time-resolved particle image velocimetry.

2. Experimental setup

In this study, we aim at characterizing the properties of positive and negative point-to-plane corona discharges. Thus, a high voltage (HV) is applied between a needle and a grounded plane electrode. Both

* Corresponding author.
E-mail address: eric.moreau@univ-poitiers.fr (E. Moreau).

https://doi.org/10.1016/j.elstat.2018.03.009
Received 31 October 2017; Received in revised form 21 March 2018; Accepted 31 March 2018

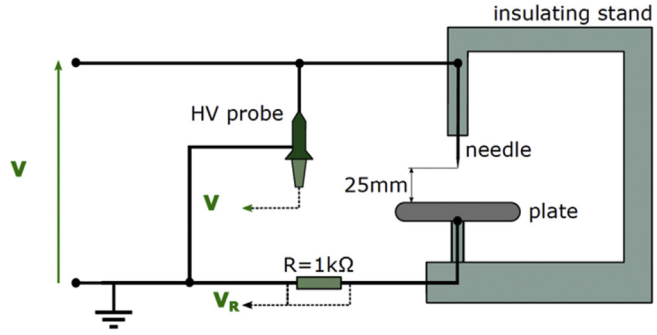

Fig. 1. Experimental setup.

electrodes are made of stainless-steel and are separated by a gap of 25 mm (Fig. 1). The needle electrode is 60 mm-long and has a tip having a curvature radius equal to 100 µm. The plane electrode has a disk shape with rounded edges and a diameter of 80 mm. Its thickness is equal to 5 mm. The high voltage is generated by a HV amplifier (Trek 30 kV/40 mA) having a slew rate of about 600 $V.\mu s^{-1}$ and is measured with a probe (North StarPVM-1, 500 MHz). The discharge current waveform is visualized with a second probe (Lecroy, PP018, 500 MHz, 10 pF) that measures the voltage across a 1 kΩ resistor set between the plate and earth. All the signals can be simultaneously recorded with a digital oscilloscope (Lecroy HDO6054, 500 MHz, 2.5 $GS.s^{-1}$). All the experiments are realized at atmospheric pressure in a few successive days. Even if temperature and pressure are quite constant during this period ($T = 22 \pm 2$ °C and $P = 1020 \pm 2$ hPa), the relative humidity could vary a little bit more ($RH = 50 \pm 15\%$). For all the experiments, the time reference t = 0 corresponds to the beginning of the high voltage rise.

Images of the discharge are recorded by a fast gateable iCCD camera (Princeton, Pi-max4 Gen2) with a resolution of 1024 × 1024 pixels [2] and equipped with a 60 mm objective. The final field of view corresponds to a 39 × 39 mm^2 region (38 µm per pixel). The same trigger source is used to synchronize all the apparatus, including the iCCD camera and the discharge ignition. The time delay between the discharge ignition and the shutter opening the camera is managed using the software of the camera (Princeton Light Field). In this study, two types of snapshots are acquired. On one hand, the shutter of the camera is triggered to open 50 µs before the beginning of the high voltage rise at t = 0 and during 200 µs (t ∈ [-50 µs, 150 µs]). One the other hand, the shutter of the camera is triggered to open 5 ms after the beginning of the high voltage rise, during 2 ms, to observe the morphology of the plasma a few milliseconds after its ignition, when the discharge is well established (t ∈ [5 ms, 7 ms]).

To characterize the ionic wind produced by the discharge, a LaVision time-resolved particle imaging velocimetry (PIV) system is used. The point-to-plane design presented in Fig. 1 is put into a PMMA tank (30 × 80 × 40 cm^3). The air is seeded with dielectric oil droplets (Ondina 915) having a mean diameter equal to 0.3 µm. A 532 nm Nd:YAG laser generator (Continuum Mesa), equipped with a divergent cylindrical lens, is used to provide a laser sheet that illuminates the particles in the x − y plane, passing through the tip of the needle and the middle of the plate (z = 0). Images are acquired using a high-speed camera (Photron Fastcam SA-Z), with a resolution of 1024 × 1024 pixels and equipped with a 60 mm lens. The resulting images have a size of 30 × 30 mm^2. The acquisition frequency is set to 20 kHz, leading to a time delay of 50 µs between two consecutive images. In total, 3000 vector fields are acquired for each experiment. The produced velocity components is computed using a cross-correlation algorithm with adaptive multi-passes, interrogation windows of 64 X 64 down to 16 X 16 pixels and an overlap set to 50%, leading to a final flow field resolution of one vector every 266 µm.

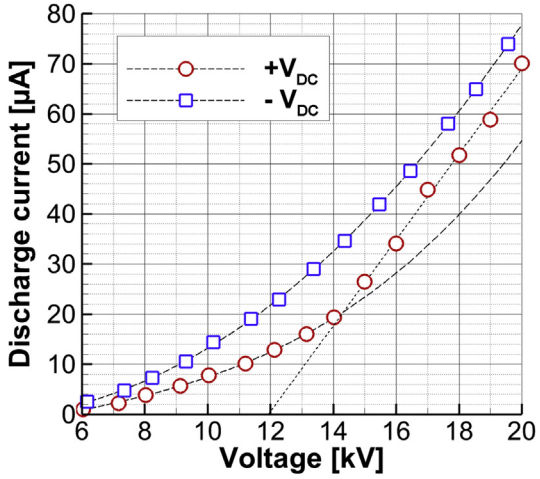

Fig. 2. Current versus voltage for positive and negative corona discharges.

3. Electrical and optical characteristics

In this section, we aim at characterizing the electrical and optical behaviors of both positive and negative discharges. First, we present current measurements and iCCD visualizations when the discharge is well established (t > 5 ms). Secondly, we focus on the transient regime of the discharge, when the high voltage is switched on (0 ≤ t ≤ 150 µs).

3.1. Steady state

Fig. 2 presents the evolution of the time-averaged discharge current versus applied high voltage, in the case of positive and negative coronas (I-V characteristics). Several remarks can be formulated. First, as expected, we can see that the negative discharge results in a higher current than the positive one. For instance, at 14 kV, the positive current is equal to 20 µA when the negative one exceeds 30 µA. Secondly, even if this kind of discharge involves complex phenomena, a simple empirical expression, called Townsend's equation, can be generally used to link the evolution of the current discharge as a function of the applied voltage V [1,3,4]:

$$I = C \times V(V - V_0) \quad (1)$$

where V is the applied DC voltage, V_0 the discharge onset voltage and C a constant depending on the voltage polarity, electrode configuration, temperature, pressure and gas composition. As we can see in Fig. 2, this equation allows us to interpolate correctly the experimental measures in the case of the negative corona. On the contrary, for the positive corona, the discharge current follows well Eq. (1) when V is equal or smaller than 14 kV, but when V becomes higher than 14 kV, the current starts to evolve linearly with the voltage. By the past, several authors have already reported some difference between the Townsend's equation and experimental measurements, these differences being observed generally at low current values and depending on the electrode geometry [38,39] or relative air humidity [40]. However, to our knowledge, it is the first time that this kind of behavior is clearly reported. Hence, in order to identify the reasons why the positive current suddenly increased when V reached 14 kV, we decided to visualize the discharge with a iCCD camera and to record the discharge current versus time (Fig. 3). These measurements should allow us to precisely characterize the different discharge regimes.

First, let us consider the case of the positive corona for which the different discharge regimes have been widely described [9,10,12,13,15,16,19]. Indeed, these studies showed that different types of corona discharge could be successively observed as the voltage increased: a burst pulse corona composed of small onset streamers, a pulseless Hermstein's glow corona, a breakdown streamer corona and